Res. Lett. Inf. Math. Sci., (2002) **3**, 199–212
Available online at http://www.massey.ac.nz/∼wwiims/research/letters/

Mathematical Modelling of Granulation: Static and Dynamic Liquid Bridges

Patrick Rynhart
I.F.S., Massey University, Palmerston North, New Zealand
P.Rynhart@massey.ac.nz
R. McKibbin
I.I.M.S., Massey University Albany Campus, Auckland, New Zealand
r.mckibbin@massey.ac.nz
R. McLachlan
I.F.S., Massey University, Palmerston North, New Zealand
r.mclachlan@massey.ac.nz
J.R. Jones
I.T.E., Massey University, Palmerston North, New Zealand
j.r.jones@massey.ac.nz

Abstract
Liquid bridges are important in a number of industrial applications, such as the granulation of pharmaceuticals, pesticides, and the creation of detergents and fine chemicals. This paper concerns a mathematical study of static and dynamic liquid bridges. For the static case, a new analytical solution to the Young-Laplace equation is obtained, in which the true shape of the liquid bridge surface is able to be written in terms of known mathematical functions. The phase portrait of the differential equation governing the bridge shape is then examined. For the dynamic case of colliding spheres, the motion of the bridge is derived from mass conservation and the Navier-Stokes equations. The bridge surface is approximated as a cylinder and the solution is valid for low Reynolds number ($\mathrm{Re} \ll 1$). As the spheres approach, their motion is shown to be damped by the viscosity of the liquid bridge.

Introduction

Granulation is an important process in the powder industry [1]. The coalescence mechanism requires that fundamental particles be bound together with a viscous binder which is able to form a liquid bridge between particles. As a result of further inter-particle collisions, primary particles adhere together forming agglomerates. As the granulation cycle continues, agglomerates bind together resulting in granules. This paper is concerned with the liquid bridges that form between fundamental particles. As an approximation, the particles are represented by spheres in this work.

A number of theoretical studies have been completed into properties of static liquid bridges which have constant physical properties [2-7]. Parameters of interest in these applications are the critical rupture distance and the area and volume of the bridge. However, approximations to the true bridge shape are introduced to solve the problem. A well-known example of this is the toroidal approximation used by Fisher [5].

Static liquid bridges are studied in the following section, and a closed form analytic solution is obtained to the Young-Laplace equation. This equation relates the curvature of the binder surface to that of the fluid surface tension and the pressure deficiency caused by the fluid droplet. Physically, this equation requires that the bridge surface has constant mean curvature. This paper shows that it is possible to represent the liquid bridge surface in terms of known Jacobi elliptic functions.

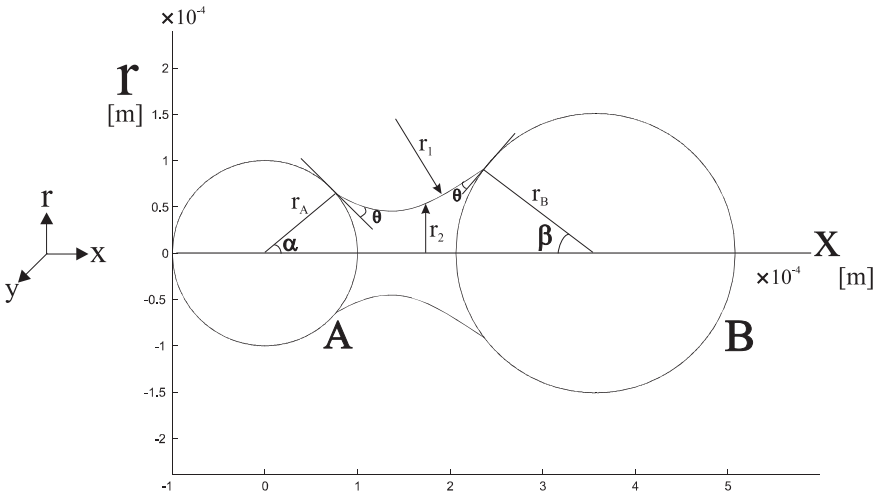

Figure 1: Illustration of the static liquid bridge geometry. Dimensional variables are used (as in equations (1) and (2)). A contact angle of $\theta = 10^{\circ}$, $\alpha = 40^{\circ}$, $\beta = 38^{\circ}$. The radius of particle A is $r_A = 0.1$ mm and particle B $r_B = 0.15$ mm. The length of the bridge is 0.12 mm.

Static Bridges

Consider figure 1 which illustrates a liquid bridge with cylindrical symmetry between two spherical particles 'A' and 'B' of radii r_A and r_B. Coordinates r and x define the position of the liquid bridge surface along with the radii of curvature r_1 and r_2 which lie in the $r-x$ and $r-y$ planes respectively. The curvature in the r-x plane is therefore given by $\frac{1}{r_1}$, and the curvature in the r-y plane by $\frac{1}{r_2}$. Allowing Δp to denote the pressure deficiency caused by the presence of the liquid droplet ($\Delta p > 0$ when the internal pressure of the bridge is higher than the external (ambient) pressure), the Young-Laplace equation relates the surface tension of the binder γ to the pressure difference Δp and the mean curvature of the bridge surface,

$$\gamma \left(\frac{1}{r_1} + \frac{1}{r_2} \right) = \Delta p. \tag{1}$$

Gravity does not appear in (1) as the mass of the liquid bridge is very small in comparison with the surface tension force between particles. Upon substitution of the vector calculus results for $\frac{1}{r_1}$ and $\frac{1}{r_2}$ (see [8] for details), equation (1) can be written

$$\gamma \left(\frac{r''}{(1+r'^2)^{3/2}} - \frac{1}{r(1+r'^2)^{1/2}} \right) = -\Delta p. \tag{2}$$

Equation (2) can be non-dimensionalised by introducing variables $X = \frac{x}{\sigma}$ and $R = \frac{r}{\sigma}$, where σ is the scaling variable relating non-dimensional and dimensional variables. In the case of figure 1, σ can be chosen as either r_A or r_B. Also, a non-dimensional pressure difference $\Delta P = \frac{\Delta p\, \sigma}{\gamma}$ is introduced, enabling the non-dimensional version of (2) to be written as

$$\frac{R''}{(1+R'^2)^{3/2}} - \frac{1}{R(1+R'^2)^{1/2}} = -\Delta P. \tag{3}$$

In (3) the notation $R' = \frac{dR}{dX}$ and $R'' = \frac{d^2R}{dX^2}$ has been adopted. Initial values for the bridge height R_0 and tangent R_0' (occurring on particle A above) are specified. The angle which the bridge makes contact with the tangent plane to the spheres is the *contact angle* θ and is specified for a given problem. The starting value for the bridge height (occurring at X_0) is

$$R_0 = \frac{r_A}{\sigma} \sin\alpha = R_A \sin\alpha$$

and that of the slope at the point of contact is

$$R_0{}' = \cot(\alpha + \theta).$$

Using the information above, an analytic solution to equation (3) is possible upon making the substitution

$$U = \left(1 + R'^2\right)^{-\frac{1}{2}}. \tag{4}$$

Differentiating U with respect to X gives

$$\frac{dU}{dX} = -\frac{R'R''}{\left(1 + R'^2\right)^{\frac{3}{2}}}. \tag{5}$$

Rearranging the right hand sides of (4) and (5), substituting these equations into (5) and applying the chain rule (where $\frac{dU}{dX}\frac{dX}{dR} = \frac{dU}{dR}$), (3) can be written as the following first order differential equation,

$$\frac{dU}{dR} + \frac{U}{R} = \Delta P. \tag{6}$$

Integrating (6) gives

$$U = \frac{R\,\Delta P}{2} + \frac{E}{R} \tag{7}$$

where the constant of integration E is the energy of the liquid bridge surface. Equation (3) defines a Hamiltonian dynamical system and hence the energy E is conserved. By combining (4) and (7),

$$E = R\left(\frac{1}{\sqrt{1 + R'^2}} - \frac{R\Delta P}{2}\right). \tag{8}$$

Substituting (4) into (7) and rearranging gives R' as

$$R' = \frac{dR}{dX} = \pm\frac{\sqrt{R^2 - \left(\frac{\Delta P\,R^2}{2} + E\right)^2}}{\frac{\Delta P\,R^2}{2} + E}$$

Rearranging the above, the shape of the bridge (where $R_0 \leq R \leq R_1$) is given by the integral

$$X = \int_{R_0}^{R} \frac{\frac{\Delta P R^2}{2} + E}{\sqrt{R^2 - \left(\frac{\Delta P R^2}{2} + E\right)^2}}\,dR. \tag{9}$$

If $E = 0$ then (9) can be solved to give

$$X^2 + R^2 = \left(\frac{2}{\Delta P}\right)^2 \tag{10}$$

showing that the liquid bridge then has a spherical shape.

If $E \neq 0$, (9) can be completed using integral tables [9]. The following parametric solution in terms of X is produced,

$$\begin{aligned} X = &\left[\mathbf{F}\left(\frac{R}{\xi}, \chi\right) - \mathbf{F}\left(\frac{R_0}{\xi}, \chi\right)\right]\left(\eta + \frac{2E}{\Delta P\,\eta}\right) \\ &+ \eta\left[\mathbf{E}\left(\frac{R_0}{\xi}, \chi\right) - \mathbf{E}\left(\frac{R}{\xi}, \chi\right)\right] \end{aligned} \tag{11}$$

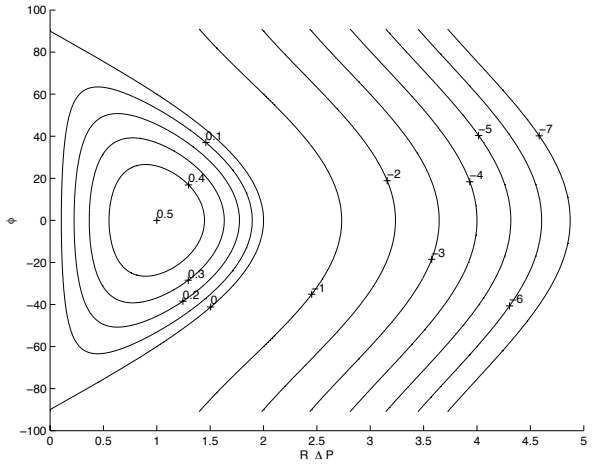

Figure 2: Phase portrait for $\Delta P > 0$. Here $\phi = \arctan R'$. Contour labels are values of $E\,\Delta P$.

where

$$\eta^2, \xi^2 = \frac{2}{(\Delta P)^2}\left[(1 - E\Delta P \pm \sqrt{1 - 2E\Delta P}\right]$$

and

$$\xi = \chi/\eta$$

such that $\xi \leq R \leq \eta$, and where $\mathbf{E}$ and $\mathbf{F}$ are Jacobi elliptic functions of the first kind [9]. Equation (11) defines the shape (R) of a bridge parameterised by the position X, where the energy levels E are determined from (8). Upon consideration of the discriminant of the the quadratic in X^2 of (9), it can be shown that $E\,\Delta P < \frac{1}{2}$.

Although equation (11) represents the liquid bridge configuration in terms of known mathematical functions, difficulty arises when attempting to integrate this solution to determine properties such as the bridge surface area and volume. In order to solve the problem in which certain properties are held constant, approximations to the bridge surface, or a numerical scheme, must be used (as in [2-6]).

Phase Portrait

The energy level E is related to the height and slope of the bridge surface (R, R') by equation (8). Boundary conditions on R and R', along with the pressure difference ΔP determine the contour for a particular liquid bridge. Generic contours, characterising all liquid bridge configurations, can be obtained from (8) by scaling. Upon introducing $\tilde{R} = R\,\Delta P$ and $\tilde{X} = X\,\Delta P$, it follows that

$$E\,\Delta P = \tilde{R}\left(\frac{1}{\sqrt{1 + \tilde{R'}^2}} - \frac{\tilde{R}}{2}\right). \tag{12}$$

An angle ϕ measured with respect to the horizontal coordinate X is introduced where $R' = \tan\phi$ and therefore $\sqrt{1 + R'^2} = \sec\phi$. In terms of ϕ, equation (12) becomes

$$E\,\Delta P = \tilde{R}\left(\cos\phi - \frac{\tilde{R}}{2}\right) \quad \text{for } \Delta P > 0, \tag{13a}$$

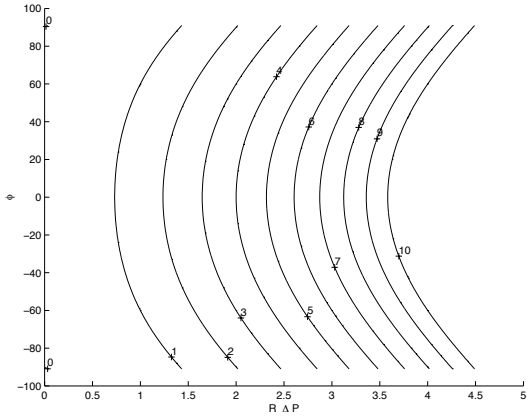

(a) Phase portrait for $\Delta P < 0$, in which $\phi = \arctan R'$ is plotted against $R\,\Delta P$. Contour labels are values of $E\Delta P$.

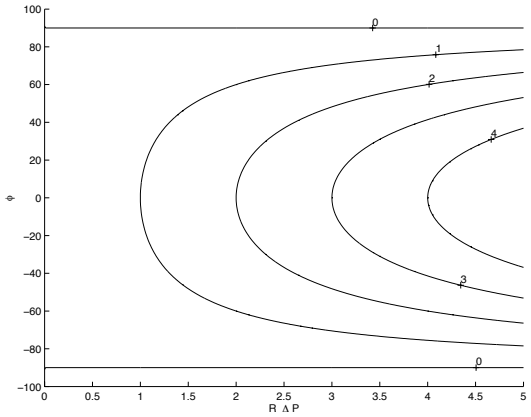

(b) Phase portrait for $\Delta P = 0$. Labels are values of E.

Figure 3: Phase portraits for $\Delta P < 0$ and $\Delta P = 0$.

$$E\,\Delta P = \tilde{R}\left(\cos\phi + \frac{\tilde{R}}{2}\right) \quad \text{for } \Delta P < 0 \tag{13b}$$

and

$$E = R\,\cos\phi \;\text{ for } \Delta P = 0. \tag{13c}$$

The phase portraits for equations (13a)-(13c) are shown in figures 2, 3(a) and 3(b). These figures show that 5 distinct types of liquid bridges exist. With reference to figure 2, for $E\,\Delta P > 0$, periodic solutions exist for $|\phi| < 90^{\text{o}}$. For this case, the shape of the liquid surface is that of a 'wavy' cylinder. For the contour $E\,\Delta P = 0.5$, $\phi \equiv 0^{\text{o}}$ and this corresponds to the cylinder solution. For $E\,\Delta P < 0$, the liquid surface begins with initial height R_0, and curves upwards reaching a maximum height $R_{\text{max}} > R_0$. The critical contour at $\phi = 90^{\text{o}}$ ($E\,\Delta P = 0$) is the sphere described in (10), which separates the cylinder and upwardly curved solutions.

When the pressure inside the bridge is equal to the external (ambient) pressure (as in figure 3(b)), two types of liquid bridges occur : for $|\phi| \neq 90^{\text{o}}$, the bridges start with initial height R_0 and then curve inward achieving a height $R_{\min} < R_0$. For $\phi = 90^{\text{o}}$, the solution corresponds to two vertical planes separated by fluid. When the pressure inside the bridge is lower than ambient ($\Delta P < 0$), the bridges curve inward as shown in figure 3(a).

Dynamic Bridges

Dynamic liquid bridges have previously been studied by Ennis *et. al* [10]. Their study was directed towards establishing the relative importance of certain dimensionless groups which govern an axially strained dynamic liquid bridge. We follow a different approach by finding a vertically averaged pressure gradient for the fluid and then the subsequent bridge motion.

Theory is presented for two general surfaces $z_1(r,t)$ and $z_2(r,t)$, as shown in figure 4, with cylindrical symmetry about the z axis separated by a gap distance $h(r,t)$. $h_0(t)$ is the closest approach distance between the surfaces, and $f_1(r)$ and $f_2(r)$ describe the shape of each surface relative to a radial datum line occurring at $z = -\frac{h_0(t)}{2}$ and $z = \frac{h_0(t)}{2}$. $z = 0$ is defined to be midway between the closest approach points of the two surfaces, which approach each other along the z axis. The particular case for two approaching spheres with a constant bridge volume V_0, as illustrated in figure 5, will then be examined.

So that the dynamics can be studied, a simple approximation is made that the shape of the bridge is a cylinder. The fluid velocity $\vec{v}$ is assumed to be steady and at low Reynolds number (Re $\ll 1$), implying that the inertial force is negligible in comparison with the viscous force of the bridge, and the fluid has constant viscosity μ. The fluid has constant and uniform density ρ (as isothermal flow is assumed), and is isotropic and incompressible. Only viscous forces are studied. No other particle interactions, such as van der Waals, surface tension, electrostatics, or the body force effect of gravity are considered.

Balance Equations

Cylindrical coordinates (r,θ,z) are used, and the velocity vector is $\vec{v} = (v_r, v_\theta, v_z)$ where v_r is the radial fluid velocity, v_θ the fluid velocity about the r-z axis, and v_z the fluid velocity in the z direction. For this system, the mass conservation equation from Hughes & Gaylord [11] is used,

$$\frac{1}{r}\frac{\partial}{\partial r}(r v_r) + \frac{\partial v_z}{\partial z} = 0 \tag{14}$$

where, by symmetry, there is no rotational flow about the z or r axes and therefore $v_\theta = 0$.

Neglecting inertial terms, that is assuming Re $\ll 1$, the momentum equations from [11] reduce to

$$0 = -\frac{\partial P}{\partial r} + \mu\left[\frac{\partial^2 v_r}{\partial r^2} + \frac{1}{r}\frac{\partial v_r}{\partial r} + \frac{\partial^2 v_r}{\partial z^2} - \frac{v_r}{r^2}\right] \tag{15}$$

$$0 = -\frac{\partial P}{\partial z} - \rho g + \mu\left[\frac{\partial^2 v_z}{\partial r^2} + \frac{1}{r}\frac{\partial v_z}{\partial r} + \frac{\partial^2 v_z}{\partial z^2}\right] \tag{16}$$

where $P = P(r, z)$ is the pressure difference between the inside and outside of the liquid bridge, defined to be positive when the pressure is higher internally. To make progress on this problem, an approximation that $v_z \ll v_r$ is introduced. Physically this means that the bridges must have a small volume, and that a small gap distance h must separate the particles when compared to the volume and radius of a fundamental particle with radius R. Since $v_z \ll v_r$, and because gravity is not considered in this approximation, only equation (15) is applicable to the solution.

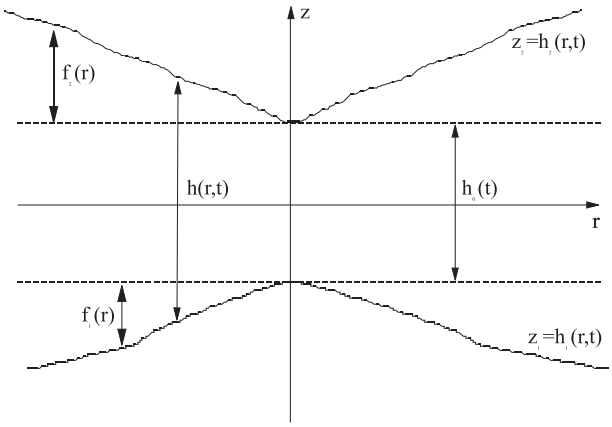

Figure 4: Figure showing two general surfaces that are approaching each other, described by $z_1 = h_1(r, t)$ and $z_2 = h_2(r, t)$, separated by a distance $h_0(t)$ which is the distance of closest approach between the two surfaces.

Velocity Profile

Consider the volume flow rate Q of fluid displaced when surfaces z_1 and z_2 move toward each other. Since the surfaces have cylindrical symmetry,

$$Q = \int_{h_1(r,t)}^{h_2(r,t)} 2\pi r\, v_r\, dz. \tag{17}$$

To determine Q, we manipulate (17) by taking the partial derivative of Q with respect to r, and then dividing through by r. Upon completing this, we obtain

$$\begin{aligned}\frac{1}{r}\frac{\partial}{\partial r}\left(\int_{h_1(r,t)}^{h_2(r,t)} 2\pi r v_r\, dz\right) &= \frac{2\pi}{r}\int_{h_1(r,t)}^{h_2(r,t)} \frac{\partial}{\partial r}(r v_r) dz \\ &+ \frac{2\pi}{r}\left(\frac{\partial h_2}{\partial r} v_r(r, h_2(r,t), t) - \frac{\partial h_1}{\partial r} v_r(r, h_1(r,t), t)\right)\end{aligned} \tag{18}$$

where the second term in (18) arises upon application of the fundamental theorem of calculus and the chain rule. Now, since the fluid is unable to move through the surfaces,

$$v_r(r, h_1(r,t), t) = v_r(r, h_2(r,t), t) = 0.$$

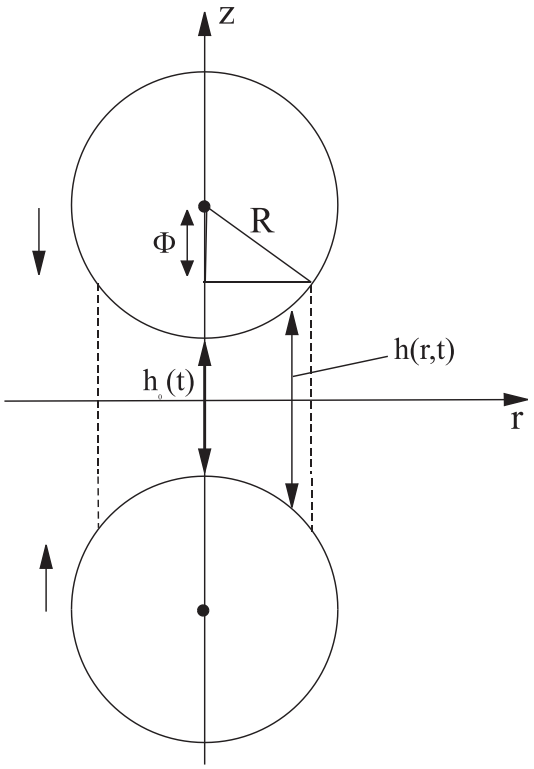

Figure 5: The scenario in which two approaching equi-sized spheres, of radius R, are connected together via a dynamic liquid bridge shown by the dotted lines.

This reduces (18) to

$$\frac{1}{r}\frac{\partial Q}{\partial r} = \frac{2\pi}{r}\int_{h_1(r,t)}^{h_2(r,t)} \frac{\partial}{\partial r}(rv_r)dz. \tag{19}$$

Substituting (14) into (19) yields

$$\begin{aligned}\frac{1}{r}\frac{\partial Q}{\partial r} &= -2\pi\int_{h_1(r,t)}^{h_2(r,t)} \frac{\partial v_z}{\partial z}dz \\ &= -2\pi\left(v_z(r,h_2(r,t),t)\right. \\ &\qquad \left. - \; v_z(r,h_1(r,t),t)\right)\end{aligned} \tag{20}$$

The separation functions $h_1(r,t)$ and $h_2(r,t)$ can be written as the sum of a time dependent function $h_0(t)$, changing as the surfaces move, and a radial function $f_1(r)$ and $f_2(r)$ as shown in figure 4. It is then possible to write $h_1(r,t) = -\frac{1}{2}h_0(t) + f_1(r)$ and $h_2(r,t) = \frac{1}{2}h_0(t) + f_2(r)$. Now

$$\begin{aligned}v_z(r,h_1(r,t),t) &= \frac{\partial h_1}{\partial t}(r=0,t) = -\frac{1}{2}\dot{h}_0(t) \\ v_z(r,h_2(r,t),t) &= \frac{\partial h_2}{\partial t}(r=0,t) = \frac{1}{2}\dot{h}_0(t),\end{aligned}$$

so it follows that equation (20) is equivalent to

$$\frac{1}{r}\frac{\partial Q}{\partial r} = -2\pi\left(\frac{1}{2}\dot{h}_0(t) - \frac{-1}{2}\dot{h}_0(t)\right) = -2\pi\dot{h}_0(t). \tag{21}$$

Therefore

$$Q(r,t) = -2\pi \int_0^r r\dot{h}_0(t)dr = -\pi r^2 \dot{h}_0(t). \tag{22}$$

For laminar flow, a parabolic radial velocity profile can be assumed,

$$v_r(r,z,t) = A(r,t)\left[z - h_1(r,t)\right]\left[h_2(r,t) - z\right] \tag{23}$$

where $A(r,t)$ is unknown and $h_1(r,t) \leq z \leq h_2(r,t)$. Substituting (23) into (17) gives

$$\begin{aligned} Q &= \int_{h_1(r,t)}^{h_2(r,t)} 2\pi r\, v_r\, dz \\ &= \int_{h_1(r,t)}^{h_2(r,t)} 2\pi r A(r,t)\left[z - h_1\right]\left[h_2 - z\right] dz \\ &= \frac{\pi r}{3} A(r,t)\left(h_2(r,t) - h_1(r,t)\right)^3 \end{aligned} \tag{24}$$

Equating (24) with (22) gives the unknown function $A(r,t) = \frac{-3r\dot{h}_0(t)}{h_2 - h_1}$, and the radial velocity profile is therefore

$$v_r(r,z,t) = \frac{-3r\left[z - h_1(r,t)\right]\left[h_2(r,t) - z\right]}{\left[h_2(r,t) - h_1(r,t)\right]^3}\dot{h}_0(t) \tag{25}$$

Equation (25) is used to find the pressure profile within the liquid bridge.

Finding the Pressure

The r momentum equation (15) is used to consider the pressure. Rearranging (15) gives

$$\frac{1}{\mu}\frac{\partial P}{\partial r} = \frac{1}{r}\frac{\partial}{\partial r}\left(r\frac{\partial v_r}{\partial r}\right) + \frac{\partial^2 v_r}{\partial z^2} - \frac{v_r}{r^2} \tag{26}$$

After differentiating (23) to find $\frac{\partial v_r}{\partial r}$ and $\frac{\partial^2 v_r}{\partial z^2}$, and substituting these results in (26), we obtain, after some tedious algebra,

$$\begin{aligned} \frac{1}{\mu}\frac{\partial P}{\partial r} = &\left[-\frac{27}{h^4}\frac{\partial h}{\partial r} + \frac{36r}{h^5}\left(\frac{\partial h}{\partial r}\right)^2 - \frac{9r}{h^4}\frac{\partial^2 h}{\partial r^2}\right] z^2\dot{h}_0 \\ &+ \left[\frac{18}{h^3}\frac{\partial h}{\partial r} - \frac{18r}{h^4}\left(\frac{\partial h}{\partial r}\right)^2 + \frac{6r}{h^3}\frac{\partial^2 h}{\partial r^2}\right] z\dot{h}_0 \\ &+ \frac{6r\dot{h}_0}{h^3} \end{aligned} \tag{27}$$

which is valid for general surfaces described by a separation function h. The radial pressure profile $\frac{\partial P}{\partial r}$ for the case of equi-sized spheres of radius R is obtained by first calculating the separation distance function $h(r,t)$, which is illustrated in figure 5. For spheres,

$$h(r,t) = h_0(t) + 2(R - \Phi)$$

where $\Phi = \sqrt{R^2 - r^2}$.
Therefore

$$h(r,t) = h_0(t) + 2\left(R - \sqrt{R^2 - r^2}\right) \tag{28}$$

Differentiating (28) gives $\frac{\partial h}{\partial r} = \frac{2r}{\sqrt{R^2-r^2}}$ and $\frac{\partial^2 h}{\partial r^2} = \frac{2R^2}{(R^2-r^2)^{\frac{3}{2}}}$. Substituting these into (27) gives

$$\begin{aligned}\frac{1}{\mu}\frac{\partial P}{\partial r} = \frac{\dot{h}_0}{(R^2-r^2)^{\frac{3}{2}}h^3}\Bigg[&\frac{54r^3-72rR^2}{h}z^2+\\ &\left(28rR^2-36r^3\right)z\Bigg]\\ &+\frac{r^3}{(R^2-r^2)h^4}\left[144\dot{h}_0z^2-72z\dot{h}_0\right]+\frac{6r}{h^3}\dot{h}_0\end{aligned} \tag{29}$$

Equation (29) includes z terms and this makes integration difficult to find the pressure P. However, since the fluid layer is small in comparison to R, the vertically averaged pressure $\bar{P}$ provides an accurate approximation. Vertical averaging, given by

$$\frac{\partial \bar{P}}{\partial r} = \frac{1}{h}\int_0^{h(r,t)}\frac{\partial P}{\partial r}\,dz, \tag{30}$$

removes the explicit z dependence, and integration to find $\bar{P}$ is then straightforward. Substitution of (29) into (30) and integrating gives

$$\frac{\partial \bar{P}}{\partial r} = \frac{6r\mu(R^2+r^2)}{h^3(R^2-r^2)}\dot{h}_0. \tag{31}$$

If the pressure of the liquid bridge at some $r = r_0$ is at ambient pressure P_{amb}, and then the bridge expands to $r > r_0$ then vertically averaged pressure is

$$\begin{aligned}\bar{P}(r,t) &= P_{\text{amb}} + \int_{r_0}^{r}\frac{\partial \bar{P}}{\partial r}dr\\ &= P_{\text{amb}} + 6\mu\dot{h}_0(t)\int_{r_0}^{r}\frac{r(R^2+r^2)}{h^3\,(R^2-r^2)}\,dr,\end{aligned}$$

and the pressure difference

$$\bar{P}(r,t) - P_{\text{amb}} = 6\mu\dot{h}_0(t)\int_{r_0}^{r}\frac{r(R^2+r^2)}{h^3\,(R^2-r^2)}\,dr. \tag{32}$$

Force

The pressure difference between the internal and external regions of the liquid bridge, $\bar{P}(r,t) - P_{\text{amb}}$, provides the force which decelerates the particles.
The force F_{bridge} is given by integrating the pressure difference over the cross-sectional area of the liquid bridge. Using equation (32), the force is

$$\begin{aligned}\text{F}_{\text{bridge}} &= m\ddot{h}_0(t)\\ &= \int_0^{r_0}\left(\bar{P}\,(r,t) - P_{\text{amb}}\right)\,dA\\ &= \int_0^{r_0}\left[2\pi\hat{r}\left(6\mu\dot{h}_0(t)\int_{r_0}^{r}\frac{\hat{r}(R^2+\hat{r}^2)}{h^3(R^2-\hat{r}^2)}\,dr\right)r\right]\,d\hat{r}\,dr\\ &= 6\pi\mu\dot{h}_0\Bigg[\int_0^{r_0}\int_0^{r}\frac{2\hat{r}(R^2+\hat{r}^2)}{h^3(R^2-\hat{r}^2)}r\,d\hat{r}dr\\ &\qquad -\int_0^{r_0}r\,dr\int_0^{r_0}\frac{2\hat{r}(R^2+\hat{r}^2)}{h^3(R^2-\hat{r}^2)}\,d\hat{r}\Bigg]\end{aligned} \tag{33}$$

i.e.

$$\ddot{h}_0 = \frac{6\pi\mu\dot{h}_0}{m}\{G\left(r_0, h_0\right) - \frac{1}{2}{r_0}^2 H\left(r_0, h_0\right)\} \tag{34}$$

where the functions

$$\begin{aligned} G(r_0, h_0) &= \int_0^{r_0}\int_0^{r} \frac{2\hat{r}(R^2+\hat{r}^2)}{h^3(R^2-\hat{r}^2)} r\, d\hat{r}dr \\ H(r_0, h_0) &= \int_0^{r_0} \frac{2r(R^2+r^2)}{h^3(R^2-r^2)}\, dr \end{aligned} \tag{35}$$

are evaluated for current radius r_0 and separation h_0. Fourth order Runge-Kutta integration (Matlab's ode45) is used to evaluate the integrals on the right hand sides of (35). (Note that the function h appearing in (35) is the separation function (28)). Once G and H are evaluated, the bridge acceleration is determined using (34).

Numerical Solution

To maintain a constant liquid bridge volume of V_0, we specify a radius r_f corresponding $h_0 = 0$ (i.e. the case where the spheres are touching). The volume to be maintained is then

$$\begin{aligned} V_0 &= \int_0^{r_f} 2\pi r\left(R - \sqrt{R^2 - r^2}\right) dr \\ &= \int_{\sqrt{R^2-r_f^2}}^{R} 2\pi\Phi\left(R - \Phi\right) d\Phi \end{aligned}$$

where the substitution $\Phi = \sqrt{R^2 - r^2}$ has been used. It follows that

$$V_0 = 2\pi\left[\frac{1}{3}(R^2 - r_f^2)^{\frac{3}{2}} + \frac{1}{2}Rr_f^2 - \frac{1}{3}R^3\right] \tag{36}$$

where V_0 is the bridge volume.

The problem begins with the initial separation $h_0(0)$ specified. As the separation distance changes, the current bridge radius r_0 changes in order to maintain the constant volume V_0. If r_0 and h_0 are the bridge radius and separation distance at time t, we are required to solve

$$V_0 = 2\pi\left[\frac{(R^2 - r_0^2)^{\frac{3}{2}}}{3} + \frac{Rr_0^2}{2} - \frac{R}{3}\right] + \pi r_0^2 h_0. \tag{37}$$

For given V_0 and h_0 there is a unique solution for r_0 which is determined numerically.

Equations (34) and (37) define a second order differential algebraic equation (DAE) subject to one constraint. Integration of (34) to obtain the bridge velocity and separation distance is achieved using a fourth order Runge Kutta integrator.

Depending on the initial values of h_0 and $\dot{h}_0$, the liquid bridge exhibits four types of behaviour. Two cases occur for $\dot{h}_0 < 0$. If a small initial gap distance separates the particles, and provided the magnitude of the initial velocity $\dot{h}_0(0)$ is sufficient, then the particles will collide. However, since the fluid has no inertia, energy is not stored in the liquid bridge and the particles do not rebound.

If the initial gap separation is too large, or the initial velocity insufficient, the bridge motion is damped by the fluid viscosity and the particles slow but do not touch. This is due to the internal pressure of the bridge

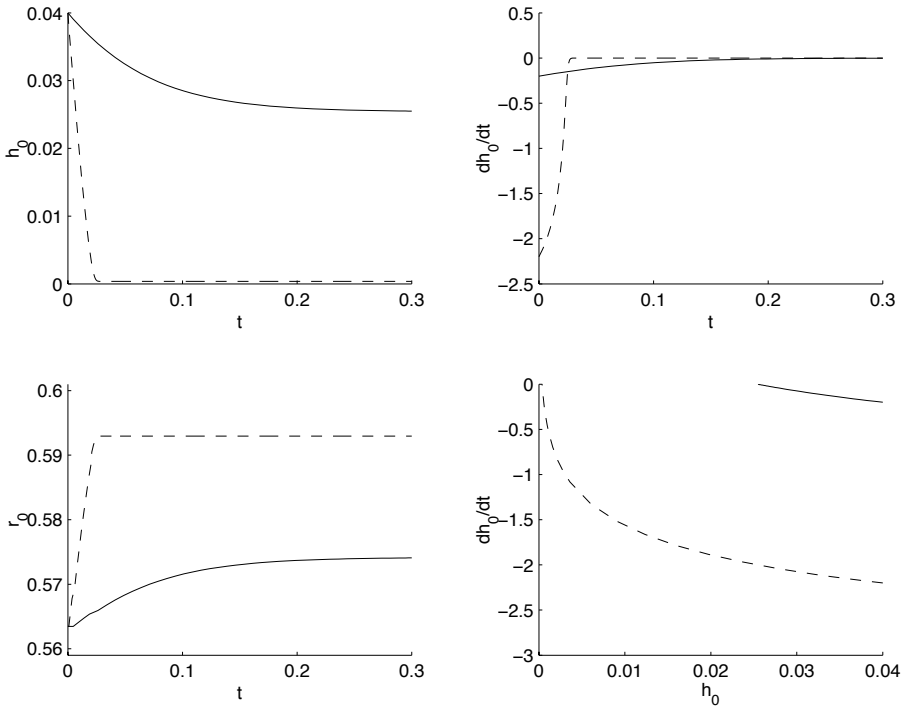

Figure 6: Two solutions from (34)-(37) are plotted for an initial separation of $h_0(0) = 0.04$ mm. The solid line case has initial particle velocity $\dot{h}_0(0) = -0.2$ mm s^{-1}, and the dashed line case $\dot{h}_0(0) = -2.2$ mm s^{-1}.

equalising to that of external (ambient) pressure. Since no pressure difference exists across the liquid bridge, the bridge force $F_{\text{bridge}} = 0$ (c.f. equation (34)) and no further particle movement occurs. Critical values for the initial separation and velocity are a function of the parameters for the problem (such as R, m and μ).

Two cases occur when the particles are initially moving away, i.e. $\dot{h}_0 > 0$. Given this initial condition, an escape velocity $\dot{h}^*$ exists such that if $\dot{h}_0(0) < \dot{h}^*$, the liquid bridge is able to retard the motion and the particles will then come to a stop. If $\dot{h}_0(0) \geq \dot{h}^*$ the particles continue to move apart.

An Example

In figure 6 two examples are shown. The dashed line plot shows two spheres approaching, slowing, and colliding. The initial conditions used are $h_0(0) = 0.04$ mm and $\dot{h}_0(0) = -2.2$ mm s^{-1}. The solid line case shows approaching spheres which do not collide, using the initial conditions $h_0(0) = 0.04$ mm, $\dot{h}_0(0) = -0.2$ mm s^{-1}. For both examples, the values of the parameters used are $R = 1$ mm, $r_0 = 0.7$ mm, $\mu = 10^{-3}$ g mm^{-1}, and particle mass $m = 0.1$ g.

Nomenclature

Static

Variable	Description	Units
r	Vertical coordinate	m
x	Horizontal coordinate	m
y	Bridge coordinate	m
θ	Contact angle	^{o}
α	Half angle for particle 'A'	^{o}
β	Half angle for particle 'B'	^{o}
Δp	Pressure difference	Pa
σ	Scaling variable	m
R	Non-dimensional bridge vertical coordinate	-
X	Non-dimensional bridge horizontal coordinate	-
ΔP	Non-dimensional pressure difference	-
E	Energy level	-

Dynamic

Variable	Description	Units
r	Vertical coordinate	m
R	Sphere radius	m
z	Vertical Coordinate	m
h	Separation function	m
h_0	Closest separation	m
$\vec{v}$	Velocity vector	$\mathrm{m\,s^{-1}}$
ρ	Fluid density	$\mathrm{kg\,m^{-3}}$
g	Acceleration due to gravity	$\mathrm{m\,s^{-2}}$
μ	Dynamic Viscosity	$\mathrm{kg\,m^{-1}}$
P	Pressure within liquid bridge	Pa
P_{amb}	Ambient pressure	Pa
$\bar{P}$	Vertically averaged pressure	Pa
Re	Reynolds number	-
F_{bridge}	Force	N
V_0	Constant bridge volume	$\mathrm{m^3}$

References

[1] Sherrington P J and Oliver R. *Granulation*. Heyden and Sons Ltd, 1981. London.

[2] Erle M A, Dyson D C and Morrow N R. Liquid bridges between cylinders, in a torus, and between spheres. *AIChE Journal*, 17(1):115–121, 1971.

[3] Lian G, Thornton M J and Adams M J. A theoretical study of the liquid bridge forces between two rigid spherical bodies. *Journal of Colloid Interface Sciences*, 161:138–147, 1993.

[4] Simons S J R and Seville J P K. An analysis of the rupture energy of pendular liquid bridges. *Chemical Engineering Sciences*, 45:2331–2339, 1994.

[5] Fisher. On the capillary forces in an ideal soil; correction of formulae given by W. B. Haines. *Journal of Agricultural Science*, 16:492–505, 1926.

[6] Willett C D, Adams M J, Johnson S A and Seville J P K. Capillary bridges between two spherical bodies. *Langmuir*, 16:9396–9405, 2000.

[7] Batchelor G K. *An Introduction to Fluid Dynamics*. Cambridge Univerisity Press, 1967. Cambridge.

[8] Hsu H P. *Applied Vector Analysis*. Harcourt Barace Jovanovic, 1984. Florida USA.

[9] Gradshteyn I S and Ryzhik I M. *Table of Integrals, Series and Products*. Academic Press, 1980.

[10] Ennis B J, Tardos G , Pfeffer R. The influence of viscosity on the strength of an axially strained pendular liquid bridge. *Chemical Engineering Science*, 45(10):3071–3088, 1990.

[11] Hughes W F and Gaylord E W. *Basic equations of Engineering Science*. McGraw-Hill, 1964.